Photonic True-Time Delay Beamformer for Broadband Wireless Access Networks at 40 GHz Band

Borja Vidal, Daniel Madrid, Juan Luis Corral, Valentín Polo, Alejandro Martínez, Jan Hendrik den Besten*, Francisco Soares*, Javier Martí, Meint K. Smit*

FRG/ITACA, Universidad Politécnica de Valencia, PO Box 22012, 46071, Valencia (Spain)
* COBRA/DIMES, Eindhoven University of Technology (The Netherlands)

Abstract — **The design parameters, sensitivity analysis and time delay measurements of a photonic true-time delay beamformer for broadband adaptive wireless access networks in the 40 GHz band are presented. The beamforming is achieved by using a multiwavelength laser in combination with a digital delay line based on optical switches and dispersive fibers.**

I. Introduction

Optical beamforming for phased-array antennas have been intensely studied during the last decade [1]-[4]. It offers many advantages such as small size, low weight, no susceptibility to electro-magnetic interference, wide instantaneous bandwidth or squint-free array steering.

In parallel, there has been a great increase in the research and deployment of broadband wireless access (BWA) networks. Several frequency bands have been allocated for it, mainly in the 28 GHz band (e.g. LMDS) and 40 GHz band (e.g. MVDS). Smart antenna technology can improve the radio performance of the above systems. Smart antennas have been traditionally controlled employing digital or IF/RF processing. These options have severe drawbacks when high-bit rate signals at millimeter-wave bands are considered. One option to overcome these limitations is optical beamforming. However, the introduction of optical beamforming in commercial applications, like wireless access networks, will require a drastic cost-reduction. In this paper, a complete architecture of a beamformer for the transmission and reception modes in a BWA network is introduced. The proposed optical beamformer has a potential low cost as it is based on mass-market wavelength-division-multiplex (WDM) technology and most of the devices are easy to integrate.

This paper is structured as follows. Section II describes briefly the optical beamformer. In section III, the design parameters for the envisaged scenario are discussed. In section IV, a sensitivity analysis on wavelength stability is presented. Some experimental results are shown in section V and, finally, conclusions are provided in section VI.

II. System Description

The optical beamforming architecture proposed in this work (see Fig. 1) is based on intensity modulation and direct detection, using 40 GHz Mach-Zehnder modulators for both transmission and reception. The beamforming is achieved by using an multiwavelength laser in combination with a digital delay line based on a fast InP-based switch matrix, as shown in Fig. 2, and dispersive fibers [5]-[6]. This architecture is based on using different simultaneous optical wavelengths with wavelength-dependent optical delay lines that introduce relative delays among the different wavelengths due to optical path dispersion. An optical wavelength-to-array element correspondence is established, so it is only needed to separate each wavelength toward its corresponding antenna. Transmission and reception paths use the same beamforming circuit, which is hence needed only once.

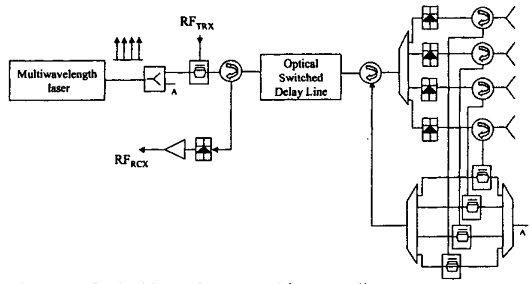

Fig. 1. Optical beamformer architecture diagram.

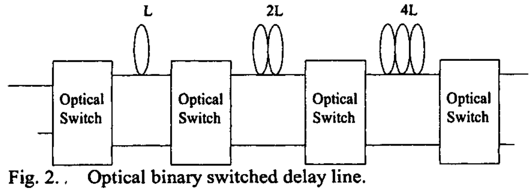

Fig. 2. Optical binary switched delay line.

The most obvious advantage of using WDM delay lines to implement time delays is that it allows to generate all the time delays for the entire array using only one switched delay line. Moreover, due to the optical wavelength-to-array element correspondence, there is no splitting loss associated with signal distribution to array elements.

The envisaged scenario for the BWA network is based on a squared cellular pattern with certain overlap and four 90 degrees sectors per cell. The duplexing approach is TDD and the multiple access method is TDMA which presents inherent benefits for highly asymmetric data services. To introduce beamforming in these networks, a space-switched single-beam antenna covering the whole sector is proposed instead of the traditional sectorial antenna. This system conception is based on actual standardization proposals [7-8]. The proposed beamformer architecture is fully compatible with this scenario where it would be placed at the base station (BS) site.

III. Design Parameters

The above scenario defines a 90 degrees sector. According to the users demands, the BS will switch between eight possible beam positions (3-bits beamformer) inside this 90 degrees sector.

If these beams were positioned with an equal angular separation, their relative position to the center of the sector will be approximately [39.4, 28.1, 16.9, 5.6, –5.6, –16.9, –28.1, –39.4] degrees. The actual beam positions will be calculated taking into account that this architecture selects the beams positions by changing the inter-element delay in a fixed amount of time delay.

If the edge beams of the sector are positioned at an angle $\pm\theta_{edge}$ relative to the center of the sector, the time excursion needed between two adjacent array elements separated by half a wavelength at a given frequency, f_{RF} in order to steer the beam between the opposite edge positions is:

$$\Delta\tau = \frac{\left|\sin\left(\theta_{edge}\right)\right|}{f_{RF}} \tag{1}$$

The optical delay unit is based on a 3-bit switched delay unit which for a given pair of wavelengths delivers eight possible delay values following the relation 0, τ, 2τ, 3τ, 4τ, 5τ, 6τ and 7τ. Therefore, the maximum delay excursion between two adjacent array elements corresponds to 7δτ where δτ, 2δτ and 4δτ are the delays that the wavelengths associated to these two adjacent elements experience when each of the three switchable optical paths are selected. Thus, the time delay precision of the architecture will be:

$$\delta\tau = \frac{\Delta\tau}{7} = \frac{\left|\sin\left(\theta_{edge}\right)\right|}{7 f_{RF}} \tag{2}$$

while the delay between adjacent array elements for each one of the three switchable optical paths will be:

$$\Delta\tau_1 = 4\delta\tau \quad \Delta\tau_2 = 2\delta\tau \quad \Delta\tau_3 = \delta\tau \tag{3}$$

For the proposed BWA scenario, the following values are selected for the edge beam position θ_{edge}=±39.4 degrees and the frequency for which the half a wavelength array separation is chosen, f_{RF} =40GHz, the system time delay precision will be:

$$\delta\tau = \frac{\Delta\tau}{7} = \frac{\left|\sin(39.4)\right|}{7\cdot 40\cdot 10^9} = 2.266\,ps \tag{4}$$

in such a way that the eight possible delays between adjacent elements will be [0, 2.27, 4.53, 6.8, 9.1, 11.3, 13.6, 15.9] ps.

In order to steer the beams to positive and negative angles relative to the center of the sector, a fixed time shift of (15.86/2) ps to each adjacent element will be included. After this correction, the eight possible delays between adjacent elements will be τ_i=[-7.9, -5.7, -3.4 –1.1, 1.1, 3.4, 5.7, 7.9] ps. These time delay increments correspond to different beam steering positions according to this expression:

$$\theta_i = \arcsin\left(2\cdot\tau_i\cdot f_{RF}\right) \tag{5}$$

In this case, the beams positions are θ_i=[-39.4, -26.9, -15.8, -5.2, 5.2, 15.8, 26.9, 39.4] degrees relative to the center of the sector.

TABLE I
Lengths of the Three Optical Paths of the TDD Unit for Different Fibers and Wavelength Separation

	Optical Path 1	Optical Path 2	Optical Path 3
Δλ =5nm Standard SMF	106.62 m	53.31 m	26.66 m
Δλ =5nm H. Dispersive SMF	25.89 m	12.95 m	6.47 m
Δλ =1nm Standard SMF	533.10 m	266.55 m	133.28 m
Δλ =1nm H. Dispersive SMF	129.47 m	64.73 m	32.37 m

Just as an example, Table I shows the needed optical path length for each bit in the optical delay unit according to previous delay calculations. Two different adjacent wavelength spacings have been considered for both standard single-mode fiber (SMF) and highly dispersive fiber.

The use of highly dispersive fiber would reduce the length of the different optical paths and the inherent difference between absolute delays for different steered angle (as an example 106.62m of SMF equals 0.5μs).

IV. Effect of the Optical Wavelength Excursion on Time Delays

Time delays based on fiber dispersion depend on the separation amongst optical wavelengths ($\Delta\lambda$) as it is shown in (6).

$$\tau = D \cdot L \cdot \Delta\lambda \qquad (6)$$

where D is the dispersion parameter of the fiber and L is the length of the optical path.

Any variation of this separation will cause a shift of the optical delays. A maximum wavelength excursion of 10% of the channel spacing is specified for the multiwavelength laser, where a nominal 5 nm separation has been defined.

Some simulations have been carried out to evaluate this effect. Time delays achieved for the -39.7 degrees beam (worst case) have been shown in Table II.

TABLE II
SIMULATION RESULTS OF THE EFFECT OF WAVELENGTH EXCURSION ON ACHIEVED DELAYS

Wavelength separation excursion	Delay between first and second elements	Delay between second and third element	Delay between third and fourth elements
Nominal wavelengths	*7.65 ps*	*7.64 ps*	*7.65 ps*
2.5% (0.125 nm)	*7.11 ps*	*8.11 ps*	*7.19 ps*
5% (0.25 nm)	*6.58 ps*	*8.67 ps*	*6.67 ps*
10% (0.5 nm)	*5.19 ps*	*10.80 ps*	*5.28 ps*

From simulation results we could assess the effect of the time delay error on the antenna array pattern. So, the residual sidelobe level (7) and the mean gain reduction (8) have been calculated [9] for a uniform linear array:

$$\overline{\sigma^2} \approx \frac{1+\overline{\Delta^2}+\overline{\delta^2}}{N} \qquad (7)$$

$$\frac{D}{D_0} \approx \frac{1}{1+\overline{\Delta^2}+\overline{\delta^2}} \qquad (8)$$

Where, $\overline{\Delta^2}$ is the amplitude error variance (in this case, it is considered to be zero), $\overline{\delta^2}$ is the phase error variance, and N is the number of elements in the array.

If isotropic elements are considered and the array phase errors follow a Gaussian probability distribution with zero mean, the values of Tables III and IV are obtained.

TABLE III
RESIDUAL SECONDARY LOBES RELATIVE TO THE MAIN LOBE

Steering angle	Residual secondary lobes relative to the main lobe		
	Wavelength Excursion 2.5%	Wavelength Excursion 5%	Wavelength Excursion 10%
39.7°	*-∞ dB*	*-∞ dB*	*-∞ dB*
27.22°	*-35.68 dB*	*-29.66 dB*	*-23.64 dB*
16.04°	*-29.66 dB*	*-23.64 dB*	*-17.62 dB*
5.45°	*-26.14 dB*	*-20.12 dB*	*-14.01 dB*
-4.95°	*-23.64 dB*	*-17.62 dB*	*-11.60 dB*
-15.51°	*-21.70 dB*	*-15.68 dB*	*-9.66 dB*
-26.66°	*-20.12 dB*	*-14.10 dB*	*-8.08 dB*
-39.05°	*-18.78 dB*	*-12.76 dB*	*-6.74 dB*

TABLE IV
VARIATION ON THE DIRECTIVITY FOR SEVERAL DIRECTIONS

Steering angle	D/D_0 (dB)		
	Wavelength Excursion 2.5%	Wavelength Excursion 5%	Wavelength Excursion 10%
39.7°	*0*	*0*	*0*
27.22°	*0.005*	*0.019*	*0.075*
16.04°	*0.019*	*0.075*	*0.291*
5.45°	*0.042*	*0.166*	*0.628*
-4.95°	*0.075*	*0.291*	*1.061*
-15.51°	*0.116*	*0.446*	*1.560*
-26.66°	*0.166*	*0.628*	*2.102*
-39.05°	*0.224*	*0.835*	*2.666*

From values reported in Tables III and IV, it can be concluded that the wavelength deviations are a critical parameter of photonic beamformers based on WDM and fiber dispersion. For the worst case steering angle (longest path) wavelength excursion will introduce a considerable degradation (-7dB for the residual sidelobe level and 2.7dB gain reduction for a 10% wavelength excursion). In this way, some care should be taken to bound this excursion in beamformers at millimeter-wave band.

V. Experimental Results

Even though the beamformer proposed in Fig.1 is aimed at BWA at 40 GHz band, its architecture is inherently RF frequency independent with a bandwidth only limited by the antenna or electrical components. Due to electrical instrument limitations, the time delays of the elemental delay line have been measured in the 2-10 GHz band. In the set-up shown in Fig. 3, the time delay is calculated from the slope of the RF phase response of the system, measured with the network analyzer by means of a frequency swept between 2 and 10 GHz. The electrical signal generated with the frequency swept in the HP8510C is used to modulate the amplitude of an optical carrier by means of a Mach Zehnder electro-optical modulator (MZM-EOM). This modulated optical signal will be delayed in the switched delay line and afterwards photodetected and entered to the HP8510C. Finally, the phase response versus frequency is measured from the phase of the S_{21} parameter.

This procedure has been carried out for four wavelengths, assuming a four element array, with a wavelength spacing of 0.8 nm. Table V shows the measured relative time delays for a 2.1- and 25.135-km-long standard single-mode fiber (SSMF) which agree quite well with the theoretical values. The difference between theoretical and measured delays could be originated from small variations between the assumed dispersion parameter of the SSMF (D=17 ps/(nm·km)) and the actual one.

TABLE V
MEASURED RELATIVE TIME DELAYS

Optical Wavelengths	2.1 km SSMF (theoretical delay: 28.56 ps)	25.135 km SSMF (theoretical delay: 341.83 ps)
1550-1550.8 nm	25.134 ps	345.01 ps
1550.8-1551.6 nm	28.4 ps	344.59 ps
1551.6-1552.4 nm	26.69 ps	345.52 ps

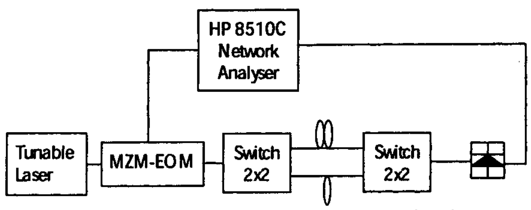

Fig. 3. Block diagram of experimental set-up for elementary switched delay line.

From previous amplitude and phase measurements (2.1 km SSMF), the antenna radiation pattern can be estimated. In Fig.4, the radiation patterns of a four element antenna with a element spacing of 0.5λ at 2 GHz have been calculated. Squint-free operation can be seen from the frequency independence of the main lobe steering angle.

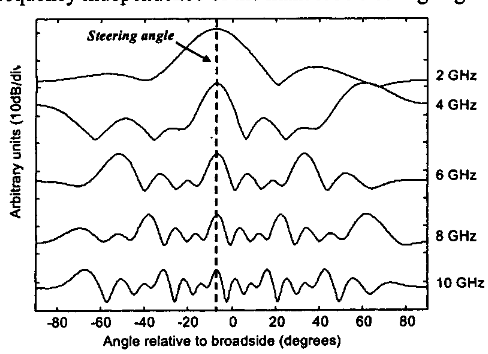

Fig. 4. Radiation pattern of a 4-element array antenna.

Finally, some measurements have been carried out to evaluate the effect of the wavelength excursion on the time delays. A 10% and 20% excursion of the wavelength spacing have been assumed and the measured delays for 2.1 km of SSMF are 23.52 ps and 15.75 ps, respectively. These values are very close to the theoretical ones (22.9 ps and 17.1 ps, respectively).

VI. CONCLUSION

Design parameters of a photonic beamformer for broadband wireless access networks in the 40 GHz band have been presented for both transmission and reception modes. The effect of the wavelength stability has been assessed, concluding that it is a critical parameter. Finally, some experimental results are presented that proved the selected approach.

ACKNOWLEDGEMENT

This work has been carried out under the framework of OBANET IST-2000-25390 project. The authors acknowledge the Spanish Research and Tech. Commission (CICYT) for funding the project TIC2000-1674.

REFERENCES

[1] W. Ng, A. Walston, G. Tangonan, J. Newberg, J.J. Lee and N. Bernstein, "The first demonstration of an optically steered microwave phased array antenna using true-time delay", *Journal of Lightwave Technology*, vol. 9, pp. 1124-1131, September 1991.
[2] R.D. Esman, M.Y. Frankel, J.L.Dexter, L.Goldberg, M.G. Parent , "Fiber optic prism true time delay antenna feed", *IEEE Photonics Technology Letters*, vol. 5, no. 11, pp.1347-1349, November 1993.
[3] H. Zmuda, E.H. Toughlian, "*Photonic aspects of modern Radar*", Ed. Artech House, 1994.
[4] I. Frigyes and A.J. Seeds, "Optically generated true-time delay in phased-array antennas"; *IEEE Trans. Microwave Theory and Tech.*, vol. 43, no. 9, pp. 2378-2386, September 1995.
[5] D.T.K. Tong and M.C. Wu, "A novel multiwavelength optically controlled phased array antenna with a programmable dispersion matrix", *IEEE Photonics Technology Letters*, vol. 8, no. 6, pp. 812-814, June, 1996.
[6] D.T.K. Tong and M.C. Wu, "Multiwavelength optically controlled phased-array antennas", *IEEE Trans. Microwave Theory and Tech*, vol. 46, no. 1, pp. 108-115, January 1998.
[7] ETSI BRAN ETR, *Broadband Radio Access Networks HIPERACCESS*, ETS 300 207-1, Nov. 1998.
[8] IEEE WirelessMAN, *Draft Standard for Air Interface for Fixed Broadband Wireless Access Systems*, IEEE 802.16.1/D1, Dec. 2000.
[9] J.L. Corral, "Application of new monolithic and photonic technologies to beam-forming networks in antenna arrays for microwave and millimetre-wave bands", *PhD. Thesis*, Universidad Politécnica de Valencia, Gandia 1998.